

# A Confocal Raman-AFM Study of Graphene

U. Schmidt,\* T. Dieing, W. Ibach, and O. Hollricher

WITec GmbH, Lise-Meitner Str. 6, 89081 Ulm, Germany

\* ute.schmidt@witec.de

## Introduction

The discovery by Novoselov and Geim [1] of a simple method to transfer a single atomic layer of carbon from the c-face of graphite to a substrate suitable for measurements of its electrical and optical properties has led to an increased interest in studying and employing two-dimensional model systems. An overview of electron and phonon properties of graphene and their relationship to the one-dimensional form of carbon known as nanotubes can be found in [2]. The unique chemical, mechanical, electrical, and optical properties of graphene lead to its many application possibilities such as: single molecule detectors, high-strength low-weight new materials, design of new semiconductor devices, etc.

An important goal however is the detection of such angstrom-thick two-dimensional sheets and precisely determining the number of layers forming the graphene flake. The aim of this contribution is to show how a confocal Raman AFM can contribute to the characterization of such small materials and devices. In the past two decades, AFM (atomic force microscopy) was one of the main techniques used to characterize the morphology of nano-materials spread on nanometer-flat substrates. From such images it is possible to gain information about the physical dimensions of the material on the nanometer scale, without additional information about their chemical composition, crystallinity, or stress state. On the other hand, Raman spectroscopy is known to be used for unequivocally determining the chemical composition of a material. By combining chemically sensitive Raman spectroscopy with high-resolution confocal optical microscopy, the analyzed material volume can be reduced below  $0.02 \mu\text{m}^3$ , leading to the ability to acquire Raman images with diffraction-limited resolution from very flat surfaces [3, 4]. Using the combination of confocal Raman microscopy with AFM, the high spatial and topographical resolution obtained with an AFM can be directly linked to the chemical information provided by confocal Raman spectroscopy [5].

## Experimental

The confocal Raman AFM alpha300 RA (www.witec.de) was used for AFM imaging in ambient conditions ( $24 \pm 2^\circ\text{C}$ ). For high-resolution topographic imaging, the AFM was operated in AC-Mode, also known as Tapping Mode. In this imaging mode the cantilever is oscillated at its resonance frequency with a free amplitude  $A_0$ . While the cantilever is approaching the surface, the oscillating amplitude is reduced to a value  $A$ , which depends on the distance to the surface. The ratio  $r = A/A_0$  defines the damping of the amplitude while the tip is in contact with the surface and is proportional to the applied force. By keeping the damping of the amplitude constant, the surface topography can be mapped. The AFM images were acquired with Arrow Force Modulation cantilevers from NanoWorld (www.nanoworld.com). The nominal spring constant of these cantilevers was 2.8 N/m, and the resonance frequency was 70–80 kHz.

For confocal Raman measurements, the alpha300 RA was equipped with a 100× (NA = 0.90) air objective and a

frequency-doubled Nd:YAG laser (excitation at 532 nm). The same graphene flake previously imaged with AFM was analyzed in Raman imaging mode. In this mode, Raman images were obtained by collecting a complete Raman spectrum at every image pixel with typical integration times below 50 ms/pixel. Spectral features (sum, peak position, peak width, etc.) were used to generate the Raman images.

## Results and Discussion

An exfoliated graphene sheet deposited on the  $\text{SiO}_2$  top layer of a Si wafer by a method described in reference 1 was examined using confocal Raman AFM. Figure 1a shows the topography of the graphene flake recorded in AFM-AC Mode. The cross section 1 highlighted in Figure 1a shows the topography variation over a bi-, mono-, and no-graphene layer. This cross section is presented in Figure 2 (top). The height difference between the  $\text{SiO}_2/\text{Si}$  wafer and the first graphene layer is  $0.8 \pm 0.2 \text{ nm}$ , whereas the double-layer of graphene is  $1.2 \pm 0.2 \text{ nm}$  high. These

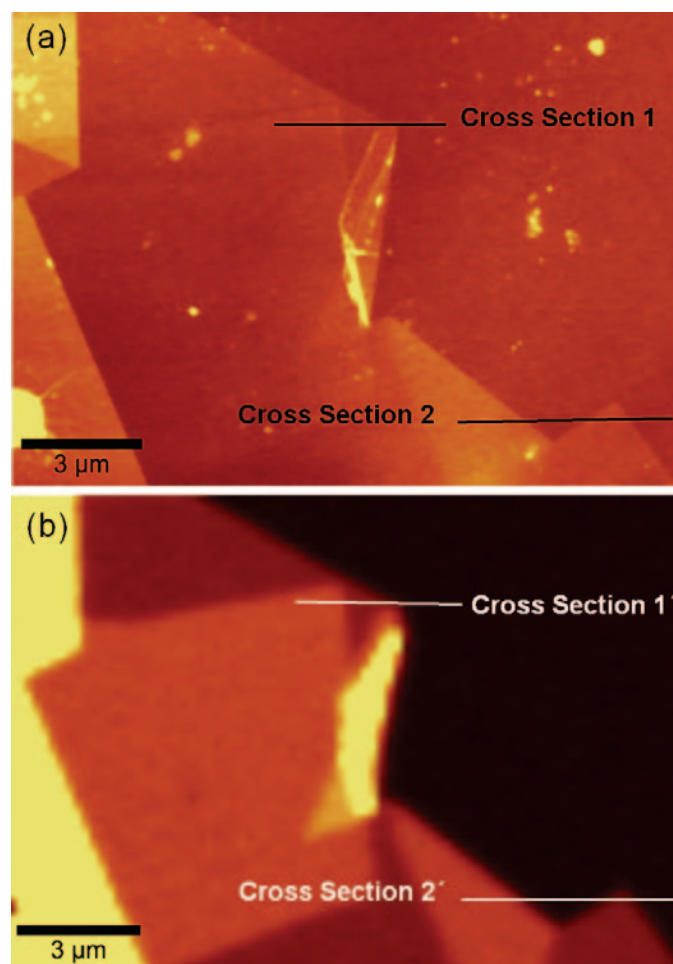
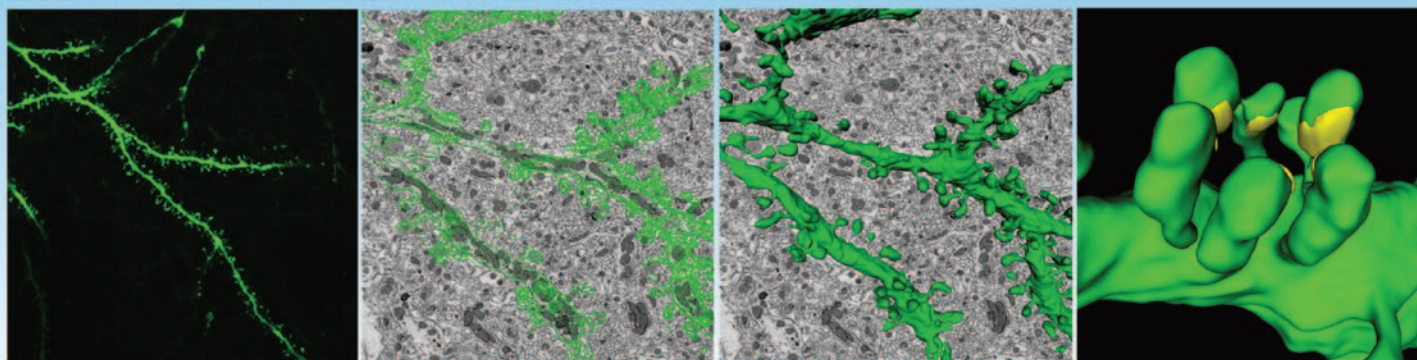
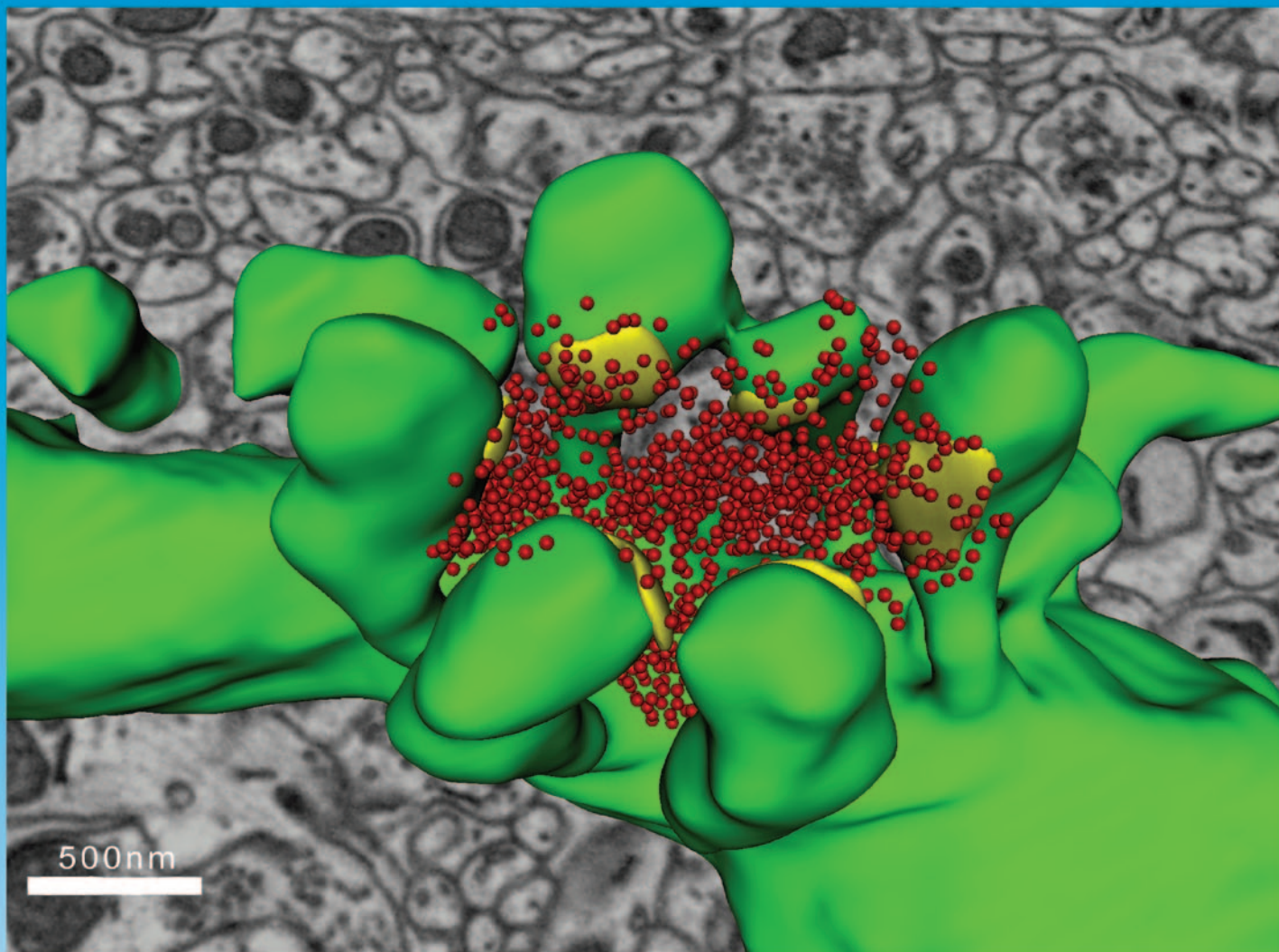


**Figure 1:** Atomic force microscope (AFM) topography image of a graphene flake (a) and Raman image of the same graphene flake showing the integrated intensity of the G-band (b).

# Complement Confocal with Ultra Resolution

https://doi.org/10.1017/S1551922511001192 Published online by Cambridge University Press



Top: A 3D reconstruction of a dendrite from a 15,625  $\mu\text{m}^3$  (25 x 25 x 25  $\mu\text{m}$ ) volumetric data set containing 500 serial images of mouse cerebellum generated by Gatan 3View<sup>®</sup>. Dendrite structure (green), buttons (yellow), and vesicles (red). Bottom Left: Confocal image of a dendrite. Middle left: 3View<sup>®</sup> image showing wire frame traces. Middle right: Wire frame traces rendered into a volumetric model. Bottom right: Ultra resolution dendritic spine model with synapses. Sample courtesy of Tom Deerinck and Dr. Mark Ellisman, National Center for Microscopy and Imaging Research, University of California, San Diego. Serial images were segmented using Imaris to create a 3D model of a neuron of interest.



ANALYTICAL TEM  
DIGITAL IMAGING  
SPECIMEN PREPARATION  
TEM SPECIMEN HOLDERS  
SEM PRODUCTS  
SOFTWARE  
X-RAY MICROSCOPY

## 3View<sup>®</sup>

Serial Block Face Imaging in the SEM

Please visit us at the 2011 American Society for Cell Biology  
Annual Meeting in Booth 641 or [www.gatan.com](http://www.gatan.com).

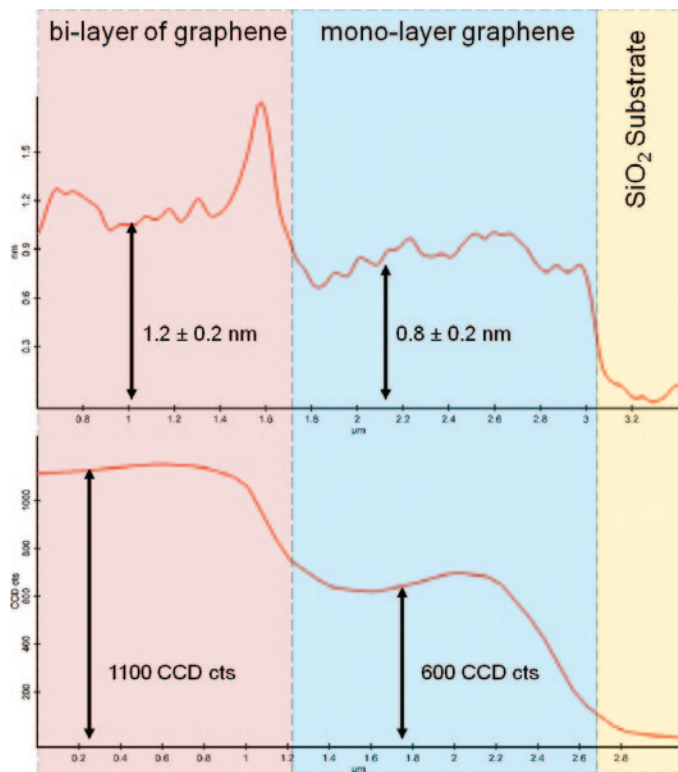


Figure 2: Signal intensity along “Cross section 1” marked in Figure 1 obtained from the AFM image (top) and Raman image (bottom).

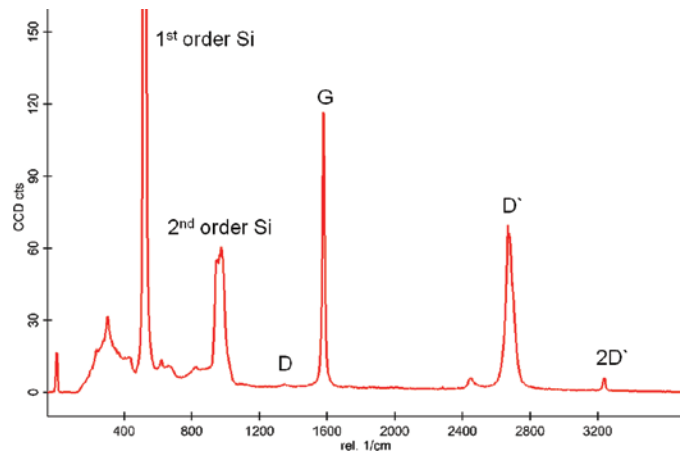


Figure 3: Averaged Raman spectrum of the analyzed graphene flake.

of a graphene flake. A more detailed analysis of the 2D array of spectra can reveal many more details about the structure of graphene. Figure 4 shows the variation of the G-band position (top), D'-band position (middle), and D'-band width as a function of number of graphene layers along cross section 1' together with the corresponding Raman images. The Raman images were obtained by a Lorenz fit of the corresponding Raman band. The position of the G-band decreases with an increasing number of graphene sheets from 1582 rel. 1/cm to 1579 rel. 1/cm due to a slightly higher frequency of the Raman active photon in graphene than in graphite [12]. The increase of the D'-band

height differences are in good agreement with previously reported AFM measurements of single and bi-layers of graphene on SiO<sub>2</sub>/Si substrates [6].

A confocal Raman image was recorded from the same sample area by acquiring a spectral array of 85 × 50 complete Raman spectra. The averaged spectrum of all recorded spectra from the array is shown in Figure 3. At low wave numbers the characteristic Raman bands of the SiO<sub>2</sub>/Si substrate are visible. The characteristic Raman bands for graphite/graphene are: the D-band (at about 1360 rel. 1/cm) characteristic for the breathing modes of sp<sup>2</sup> bonded atoms in rings and the G-band (at about 1580 rel. 1/cm) due to bond stretching of sp<sup>2</sup> bonded atoms in chains and rings [7–9]. In graphene two additional Raman bands, D' (around 2700 rel. 1/cm) and 2D' (around 3250 rel. 1/cm), are observed, which are both due to second-order resonant phonon Raman scattering [2]. The image in Figure 1b shows the integrated intensity of the G-band from the 2D spectral array. It can be seen that the integrated intensity of the G-band varies proportionally with the number of graphene sheets [10, 11]. A cross section 1' along the same sample position as in the topography image is shown in Figure 2 (bottom). This image already indicates that Raman microscopy, a fast, non-contact imaging method, can give insight into the composition

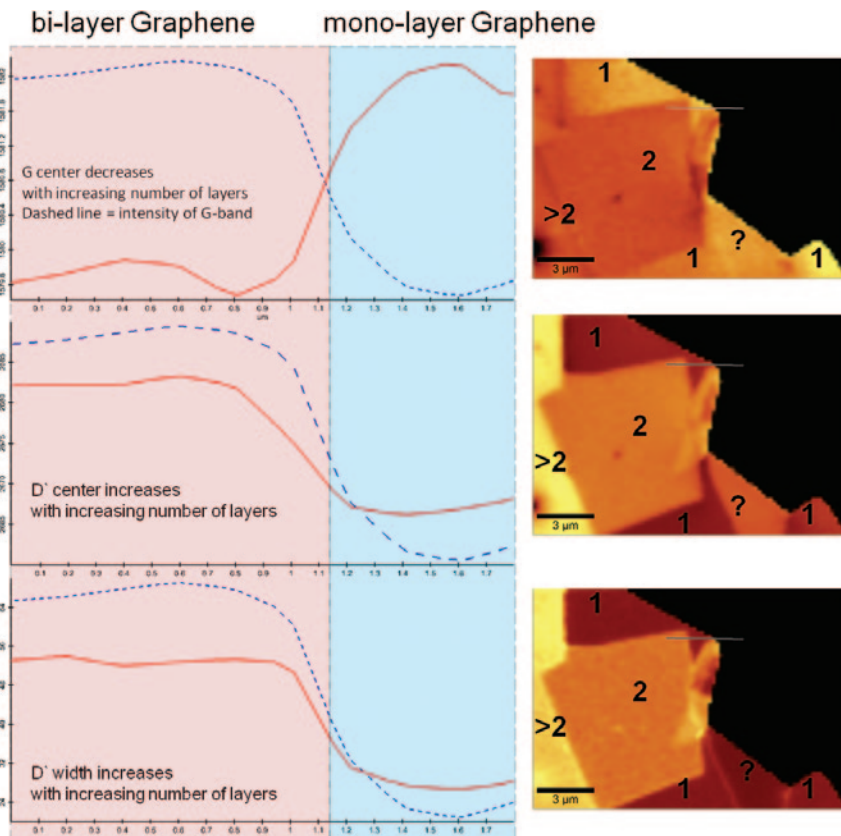


Figure 4: Variation of the position of the G-band (top left), D'-band (middle left), and width of D'-band (bottom left) along “Cross Section 1” marked in Figure 1 without the SiO<sub>2</sub>/Si substrate and the corresponding Raman images of the analyzed graphene flake (right column).

**Table 1:** Summary of measured data obtained along cross section 2 from the AFM topography image and various Raman images recorded from the same sample area shown in Figure 1.

Number of graphene layers	Step height measured with AFM [nm]	Integrated intensity of G-band [CCD cts]	Center of G-band [rel. 1/cm]	Center of D'-band [rel. 1/cm]
1	$0.9 \pm 0.2$	$524 \pm 10$	$1583 \pm 1$	$2672 \pm 1$
1 or 2?	$2.00 \pm 0.2$	$1072 \pm 10$	$1583 \pm 1$	$2679 \pm 1$

position and D'-band width with increasing number of graphene layers is due to strong electron-phonon coupling in single and bi-layers of graphene [2, 10–12]. Based on these results, one can assign the number of layers that form the studied graphene flake. Numbers in the Raman images in Figure 4 indicate the number of graphene layers. An inconsistency however can be seen in the area marked with a question mark. In this area the position of the G-band shows the presence of one graphene layer, however the Raman image obtained from the Lorenz fit of the position of the D'-band (Figure 4 middle), the integrated intensity of the G-band (Figure 1b), and the AFM image (Figure 1a) show the presence of at least two graphene layers. The data measured from cross sections along section 2 and 2' in the AFM topography image (Figure 1a), the Raman images of the intensity of G-band (Figure 1b), position of G-band (Figure 4 top right), center of D'-band (Figure 4 middle right) are summarized in Table 1. The inconsistency described above may arise from a flipped-over, decoupled part of the graphene layer. One can clearly see that the topography of this double layer is in good agreement with the double height of a single layer of graphene deposited on a SiO<sub>2</sub>/Si substrate. A similar result is obtained from the integrated intensity of the G-band, showing clearly the presence of two graphene layers. Nevertheless, the center position of the G and D'-bands clearly show the properties of a single, loose graphene layer.

### Summary

The combination of a confocal Raman microscope with an AFM was used for the characterization of a graphene flake. The AFM image reveals the topographic structure of the graphene flake with a sub-nanometer z-resolution. From this image it is possible to determine the number of graphene layers in the graphene flake.

Raman spectroscopy allows the identification of chemically different materials or different properties within a material. Graphene flakes consisting of single or bi-layers of graphene of sub-nanometer height provide a strong Raman signal because

of their special electronic and photonic properties. The Raman signal is very sensitive to the number of graphene layers, thus Raman imaging of graphene flakes provides a fast and detailed description of the structure of graphene.

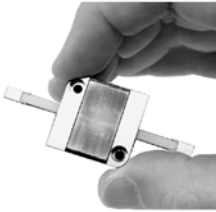
### References

- [1] KS Novoselov, AK Geim, SV Morozov, D Jiang, Y Zhang, SV Dubonos, IV Grigorieva, AA Firsov, *Science* 306(5696) (2004) 666.
- [2] JC Charlier, PC Eklund, J Zhu, and AC Ferrari, "Electron and phonon properties of graphene: their relationship with carbon nanotubes" in A Jorio, G Dresselhaus, and MS Dresselhaus, *Carbon Nanotubes: Advanced Topics in the Synthesis, Structure, Properties and Applications, Series: Topics in Applied Physics 111*, Springer-Verlag, New York, 2008, 673–709.
- [3] P Lasch, A Hermelink, and D Naumann, *Analyst* 1–9 (2009).
- [4] A Jungen, VN Popov, C Stampfer, C Durrer, S Stoll, and C Hierold, *Physical Review* 75(405) (2007).
- [5] U Schmidt, S Hild, W Ibach, and O Hollricher, *Macromol Symp* 230(133) (2005).
- [6] M Ishigami, JH Chen, WG Cullen, MS Fuhrer, and ED Williams, *Nano Lett* 7 (2007) 1643.
- [7] C Castiglioni, F Negri, M Rigolio, G Zerbi, *J Chem Phys* 115 (2001) 3769.
- [8] F Tuinstra and J Koenig, *J Chem Phys* 53 (1970) 1126.
- [9] AC Ferrari and J Robertson, *Phys Rev B* 61 (2000) 14095.
- [10] D Graf, F Molitor, K Ensslin, C Stampfer, A Jungen, C Hierold, and L Wirtz, *Eur Phys J Special Topics* 148 (2007) 171–76.
- [11] Yy Wang, Zh Ni, T Yu, ZX Shen, Hm Wang, Yh Wu, W Chen, and ATS Wee, *J Phys Chem C* 112 (2008) 10637–40.
- [12] S Piscanec, M Lazzeri, F Mauri, A Ferrari, and J Robertson, *Phys Rev Lett* 93 (2004) 185503.

MT

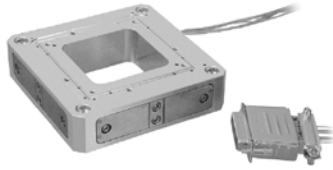
## Non-Magnetic Piezo Motors / Scanners

FOR SCANNING PROBE MICROSCOPY




**Non-Magnetic Linear Motors**

- + Sub-nm Resolution
- + High Force / High Speed



**Piezo Flexure Stages, 1 to 6 Axis**

- + Sub-nm Precision, Fast Response
- + To 1.8 mm Travel, Low Profile



**Fast AFM Scanning Stages**

- + Picometer Resolution
- + Closed-Loop Control

# PI

Whether in microscopy, optical metrology or adaptive optics—PI's compact piezoelectric systems provide a unique combination of dynamics, precision and reliability.

PI (Physik Instrumente) LP  
508.832.3456 info@pi-usa.us  
[www.pi.ws/mt](http://www.pi.ws/mt)

ITAR Certified  
USA Custom Design/Build

